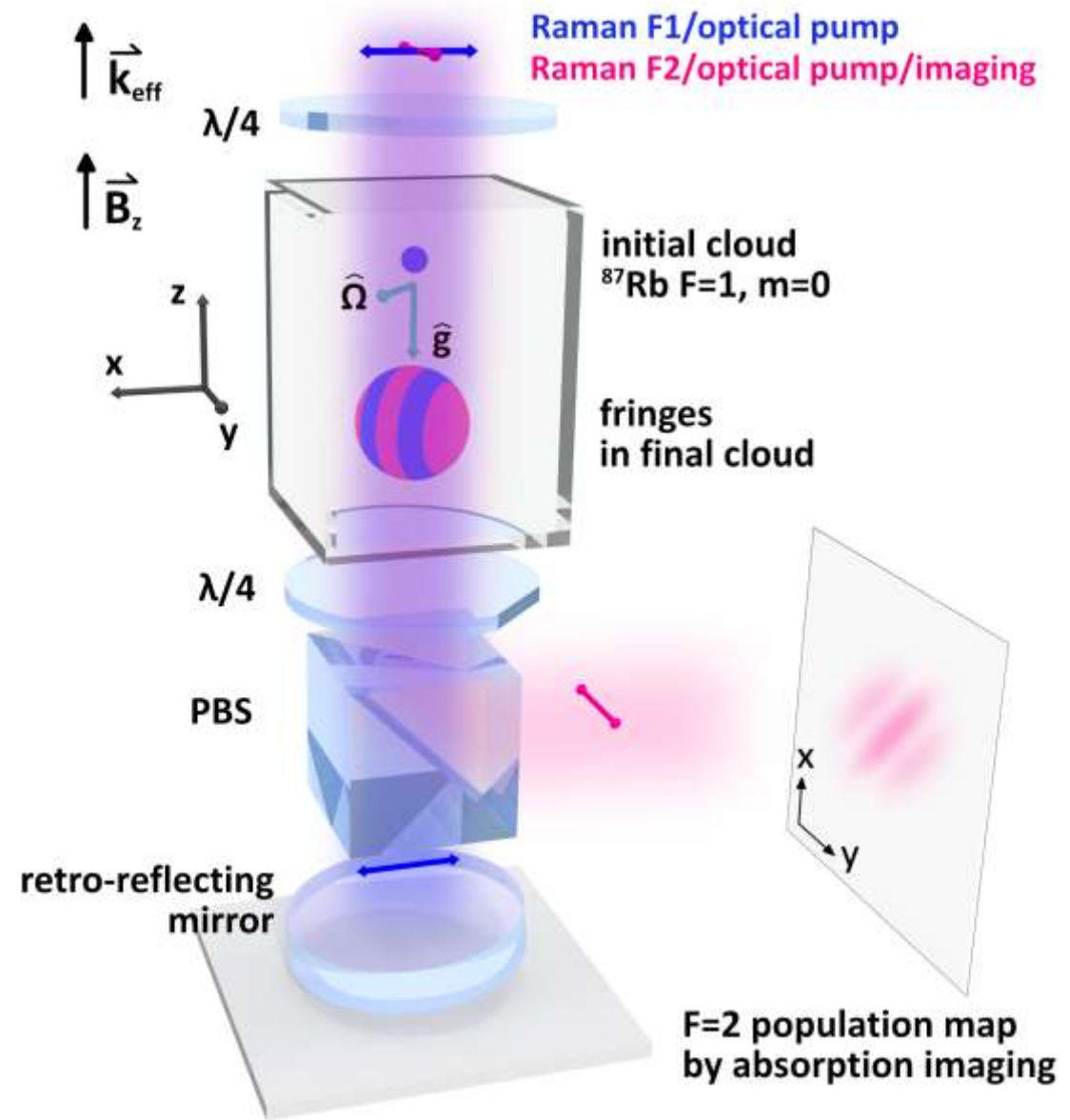


Inertial sensing with point-source atom interferometry for interferograms with less than one fringe

Yun-Jhii Chen^{1,2}, Azure Hansen¹,
Moshe Shuker^{1,3}, Rodolphe Boudot^{1,4},
John Kitching¹, and Elizabeth A. Donley¹

1. National Institute of Standards and Technology, Boulder, CO 80305 USA
2. University of Colorado, Boulder, CO 80309 USA
3. Rafael Ltd. (Israel)
4. FEMTO-ST, CNRS, 26 Rue de l'Epitaphe, 25030, Besançon, France



Rotation measurement with interferometry

"The Feynman path integral approach to atomic interferometry. A tutorial," Pippa Storey and Claude Cohen-Tannoudji, Journal de Physique II, EDP Sciences, 1994, 4 (11), pp.1999-2027.

Sagnac phase shift

$$\delta\varphi_{\text{photon}} = \frac{2\omega_0}{c^2} A\Omega \quad \text{Light wave}$$

$$\delta\varphi_{\text{atom}} = \frac{2M}{\hbar} A\Omega \quad \text{Matter wave}$$

A: Sagnac area

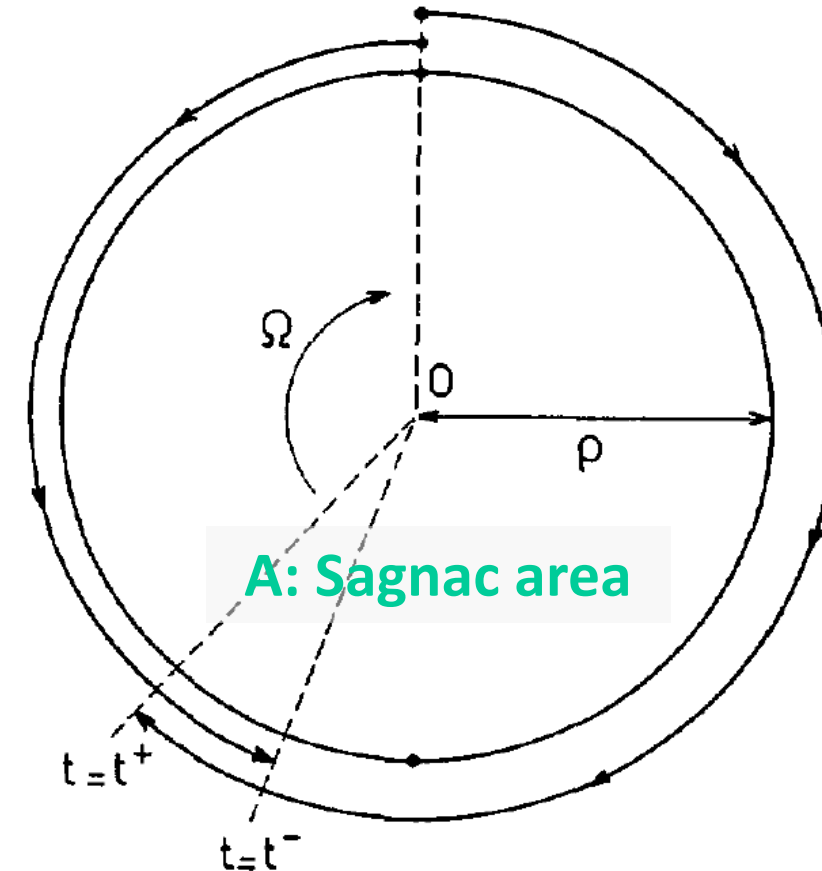
Ω : rotation rate

M: mass of atom

ω_0 : angular frequency of light

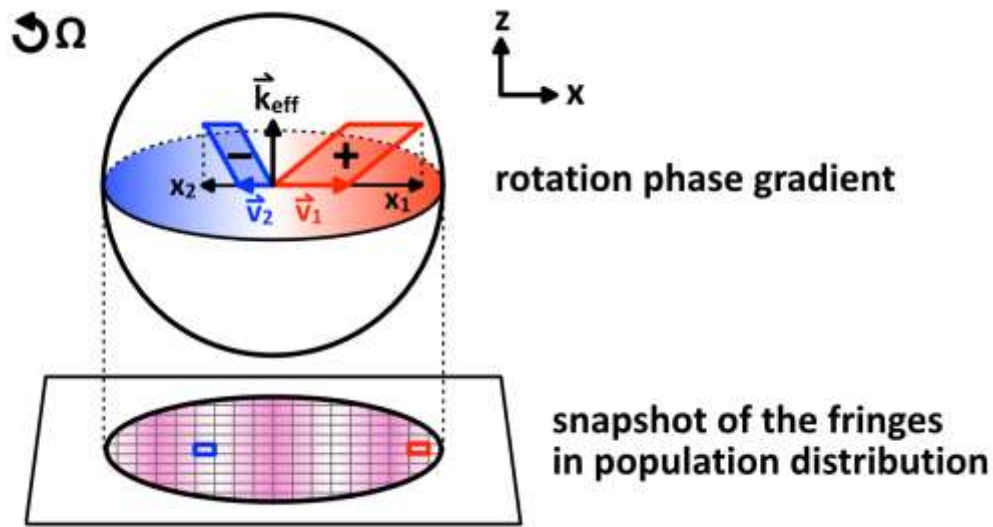
c: speed of light

\hbar : reduced Plank constant



Point source atom interferometry (PSI)

1. PSI is a parallel operation of many different Sagnac interferometers.
2. PSI enables direct rotation measurement without ambiguity.
3. PSI resolves a rotation vector in a plane with high dynamic range.



$$\varphi_{\Omega} = \frac{2m}{\hbar} \vec{\Omega} \cdot \vec{A} \quad \text{rotation phase}$$

A: Sagnac area (depends on atom velocity)

Acknowledgement

Rodolphe Boudot

Liz Donley

Azure Hansen

Greg Hoth

Eugene Ivanov

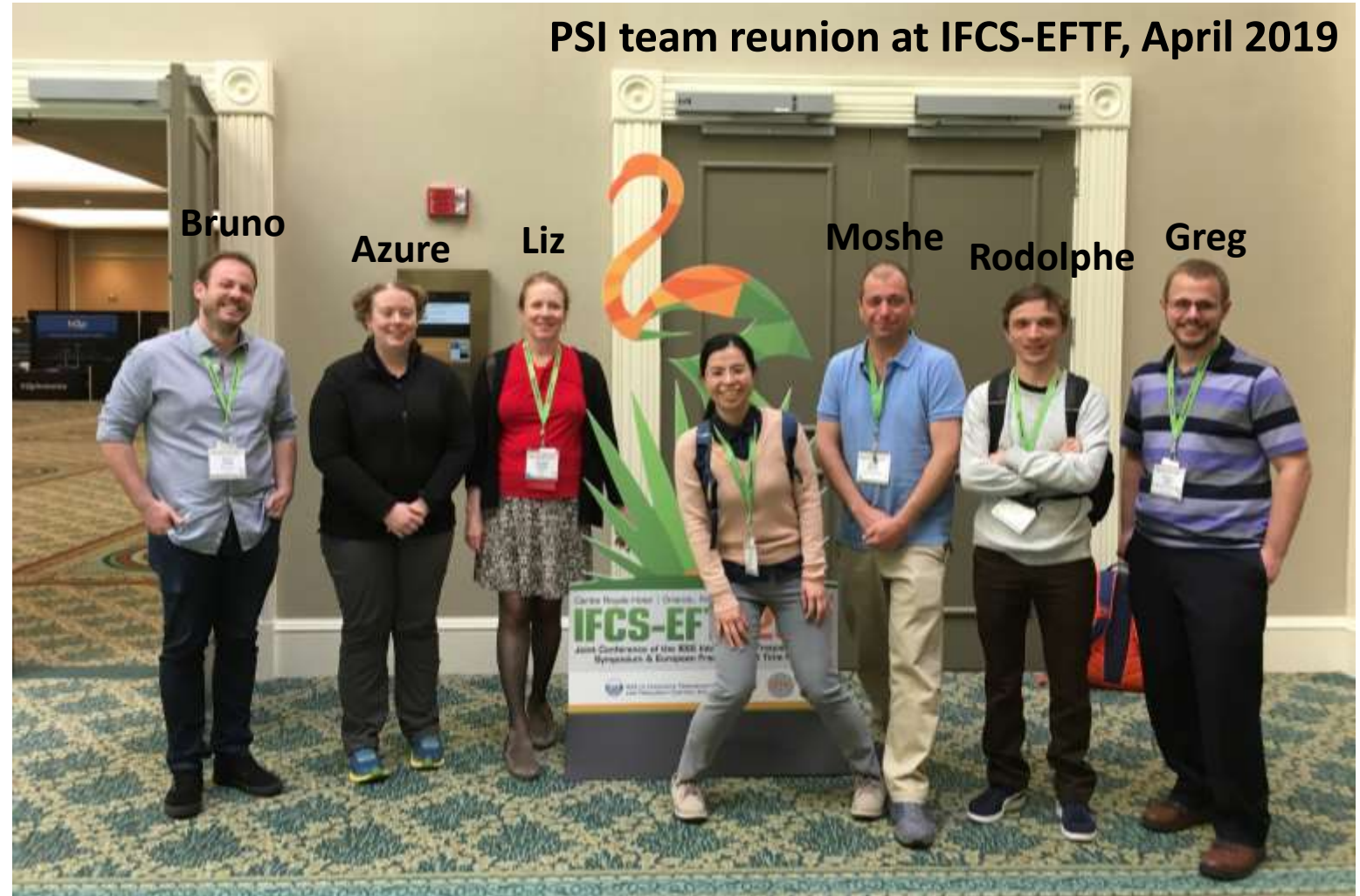
John Kitching

William McGehee

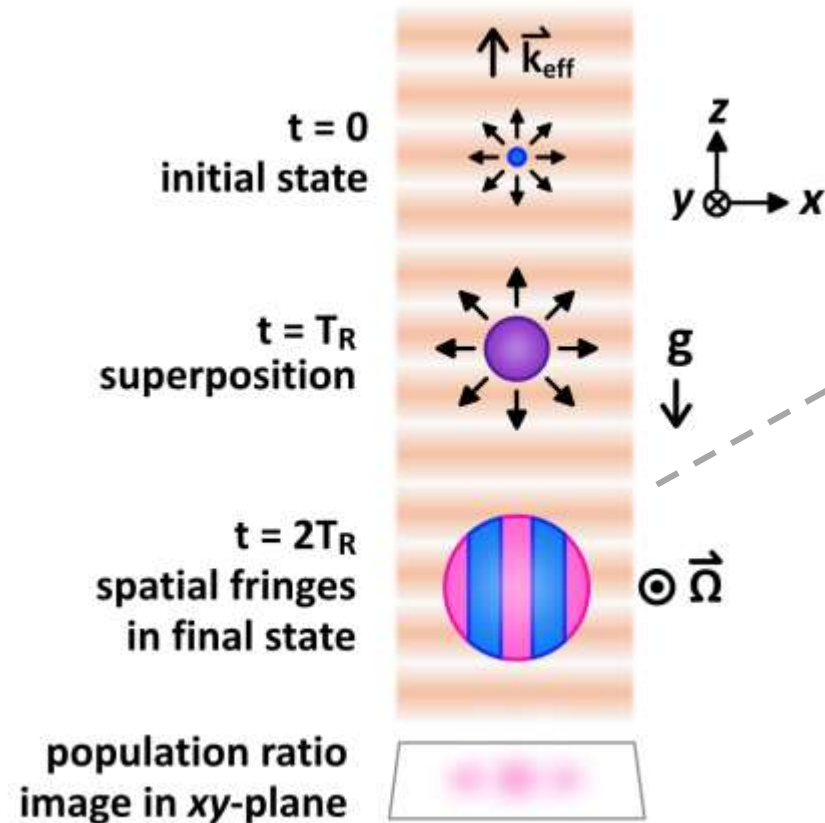
Bruno Pelle

Stefan Riedl

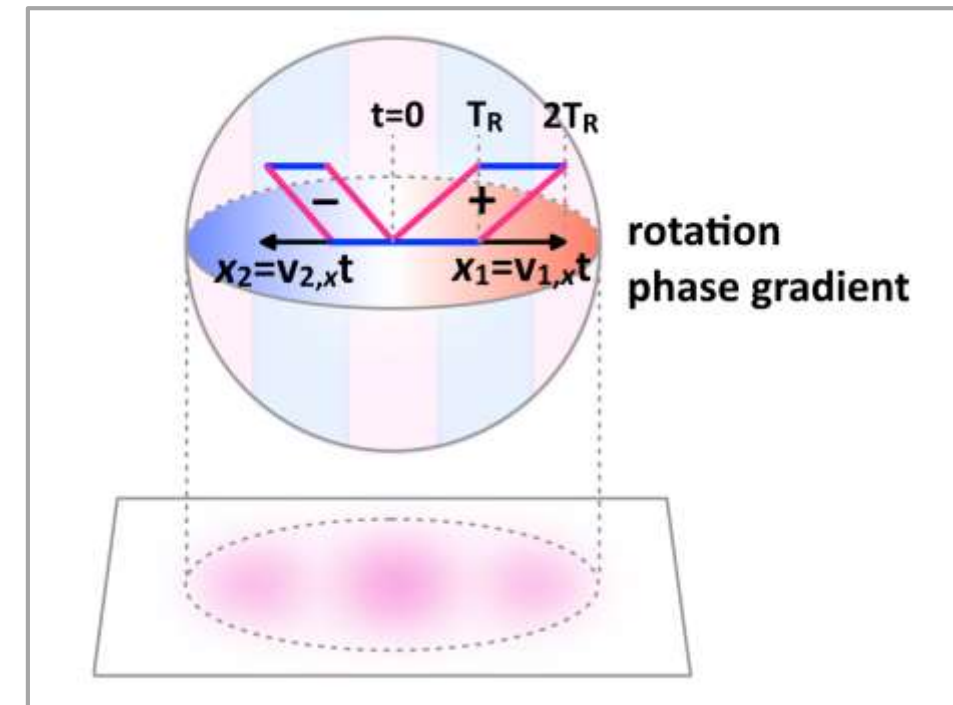
Moshe Shuker



Expanding point-like atomic source



Different velocity classes are mapped to different locations in the image plane with the position-velocity correlation of a point source.



Rotation phase gradient

Interferometer phase shift of the Raman $\pi/2-\pi-\pi/2$ pulse sequence:
 $\varphi = \varphi_a + \varphi_0 + \varphi_\Omega$
 $\varphi_a = \vec{k}_{\text{eff}} \cdot \vec{a} T_R^2$ acceleration
 $\varphi_\Omega = 2\vec{k}_{\text{eff}} \cdot (\vec{\Omega} \times \vec{v}) T_R^2$ **velocity dependent!**
 φ_0 = laser phase
 T_R : time between Raman laser pulses

Position-velocity correlation of an **ideal** expanding point source: $\vec{v} = \frac{\vec{r}}{T_{\text{ex}}}$
 T_{ex} : cloud expansion time



$\varphi_\Omega(\vec{r}) = \vec{k}_\Omega \cdot \vec{r}$ **rotation phase gradient**
 $\vec{k}_\Omega = \frac{2T_R^2}{T_{\text{ex}}} k_{\text{eff}} \Omega \hat{n}$
 $\hat{n} = \vec{k}_{\text{eff}} \times \vec{\Omega}$
 φ_a and φ_0 : constant across cloud

- Fringe period : rotation rate
- Fringe direction : direction of the rotation vector
- Fringe phase : acceleration

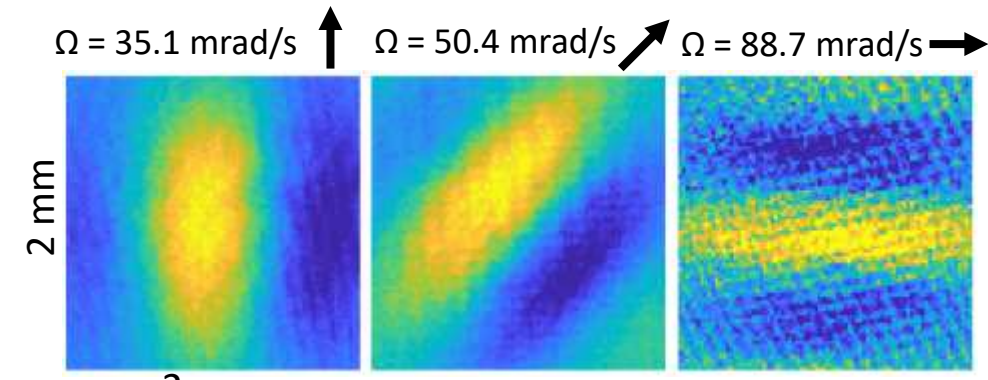


Image plane is transverse to \vec{k}_{eff}

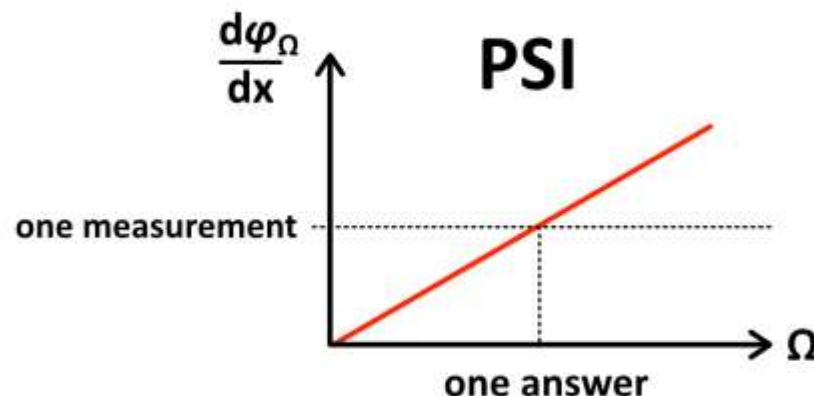
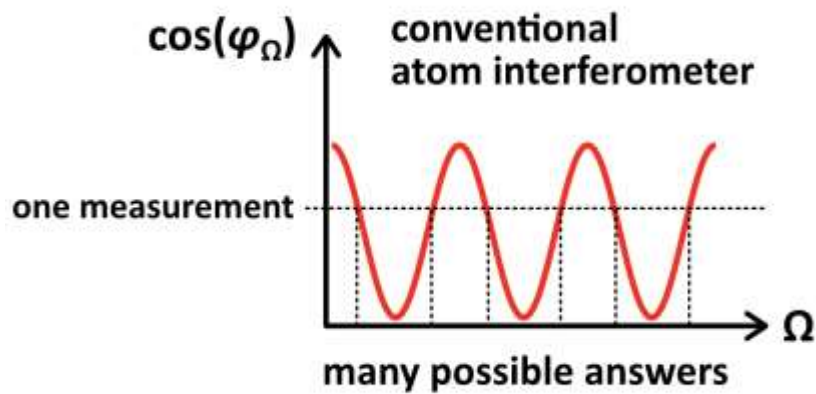
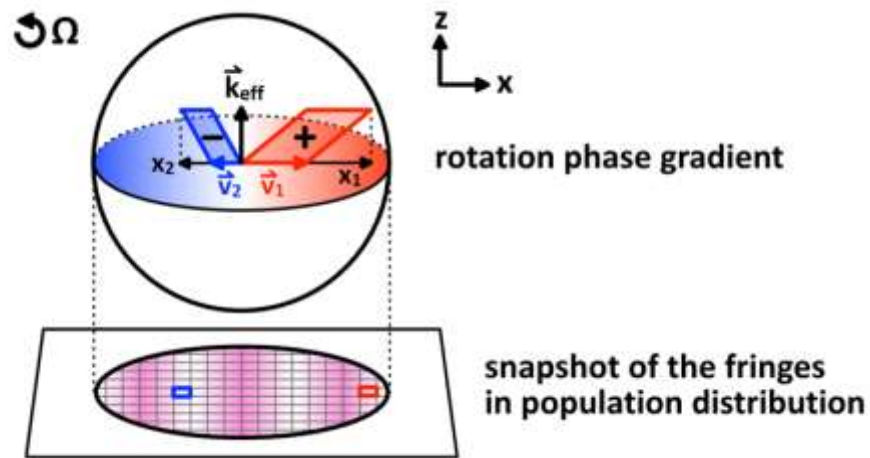
Unambiguous rotation measurement

Conventional:

Population ratio \rightarrow phase \rightarrow rotation

PSI:

Fringe period \rightarrow phase gradient \rightarrow rotation



PSI references

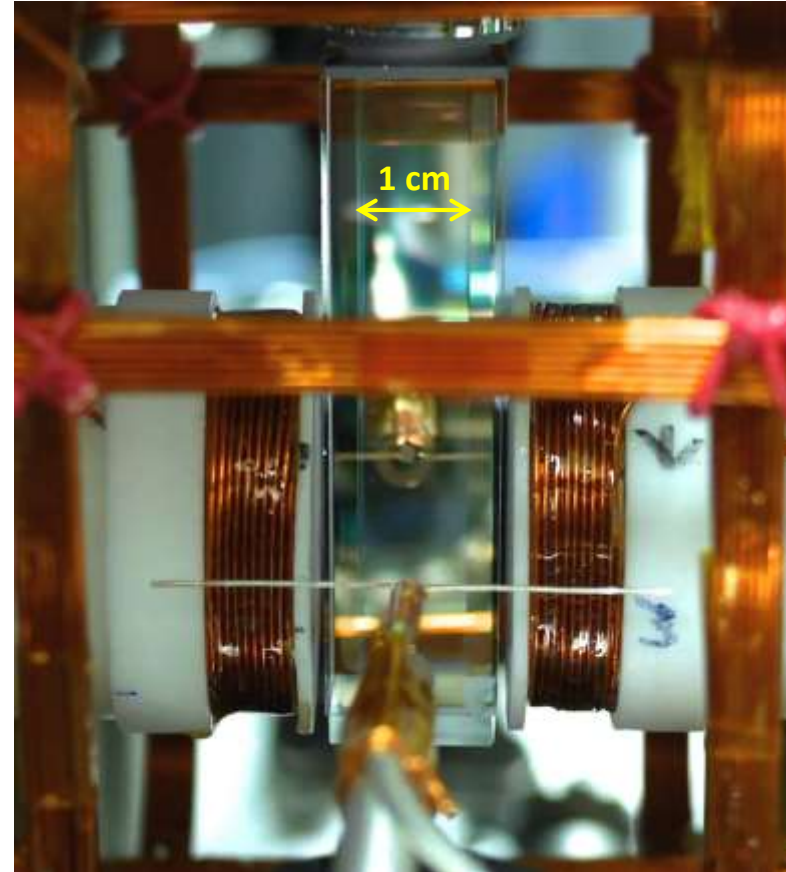
	Authors	Link	Year
Multiaxis inertial sensing with long-time point source atom interferometry	Susannah M. Dickerson, Jason M. Hogan, Alex Sugarbaker, David M. S. Johnson, and Mark A. Kasevich	https://doi.org/10.1103/PhysRevLett.111.083001	2013
Enhanced Atom Interferometer Readout through the Application of Phase Shear	Alex Sugarbaker, Susannah M. Dickerson, Jason M. Hogan, David M. S. Johnson, and Mark A. Kasevich	https://doi.org/10.1103/PhysRevLett.111.113002	2013
Point source atom interferometry with a cloud of finite size	Gregory W. Hoth, Bruno Pelle, Stefan Riedl, John Kitching, and Elizabeth A. Donley	https://doi.org/10.1063/1.4961527	2016
Single-source multiaxis cold-atom interferometer in a centimeter-scale cell	Yun-Jhih Chen, Azure Hansen, Gregory W. Hoth, Eugene Ivanov, Bruno Pelle, John Kitching, and Elizabeth A. Donley	https://doi.org/10.1103/PhysRevApplied.12.014019	2019
Concept study and preliminary design of a cold atom interferometer for space gravity gradiometry	A. Trimeche, B. Battelier, D. Becker, A. Bertoldi, P. Bouyer, C. Braxmaier, E. Charron, R. Corgier, M. Cornelius, K. Douch, N. Gaaloul, S. Herrmann, J. Müller, E. Rasel, C. Schubert, H. Wu and F. Pereira dos Santos	https://doi.org/10.1088/1361-6382/ab4548	2019
Rotation sensing with improved stability using point-source atom interferometry	Chen Avinadav, Dmitry Yankelev, Moshe Shuker, Ofer Firstenberg, and Nir Davidson	https://doi.org/10.1103/PhysRevA.102.013326	2020
A Multi-Axis Atom Interferometer Gyroscope Based on a Grating Chip	Xiaojie Li, Zhixin Meng, Peiqiang Yan, Jianwei Zhang, Yanying Feng	https://doi.org/10.1109/INERTIAL48129.2020.9090092	2020
High sensitivity multi-axes rotation sensing using large momentum transfer point source atom interferometry	Jinyang Li, Gregório R. M. da Silva, Wayne C. Huang, Mohamed Fouda, Timothy L. Kovachy, and Selim M. Shahriar	https://arxiv.org/abs/2006.13442	2020
Robust inertial sensing with point-source atom interferometry for interferograms spanning a partial period	Yun-Jhih Chen, Azure Hansen, Moshe Shuker, Rodolphe Boudot, John Kitching, and Elizabeth A. Donley	https://doi.org/10.1364/OE.399988	2020

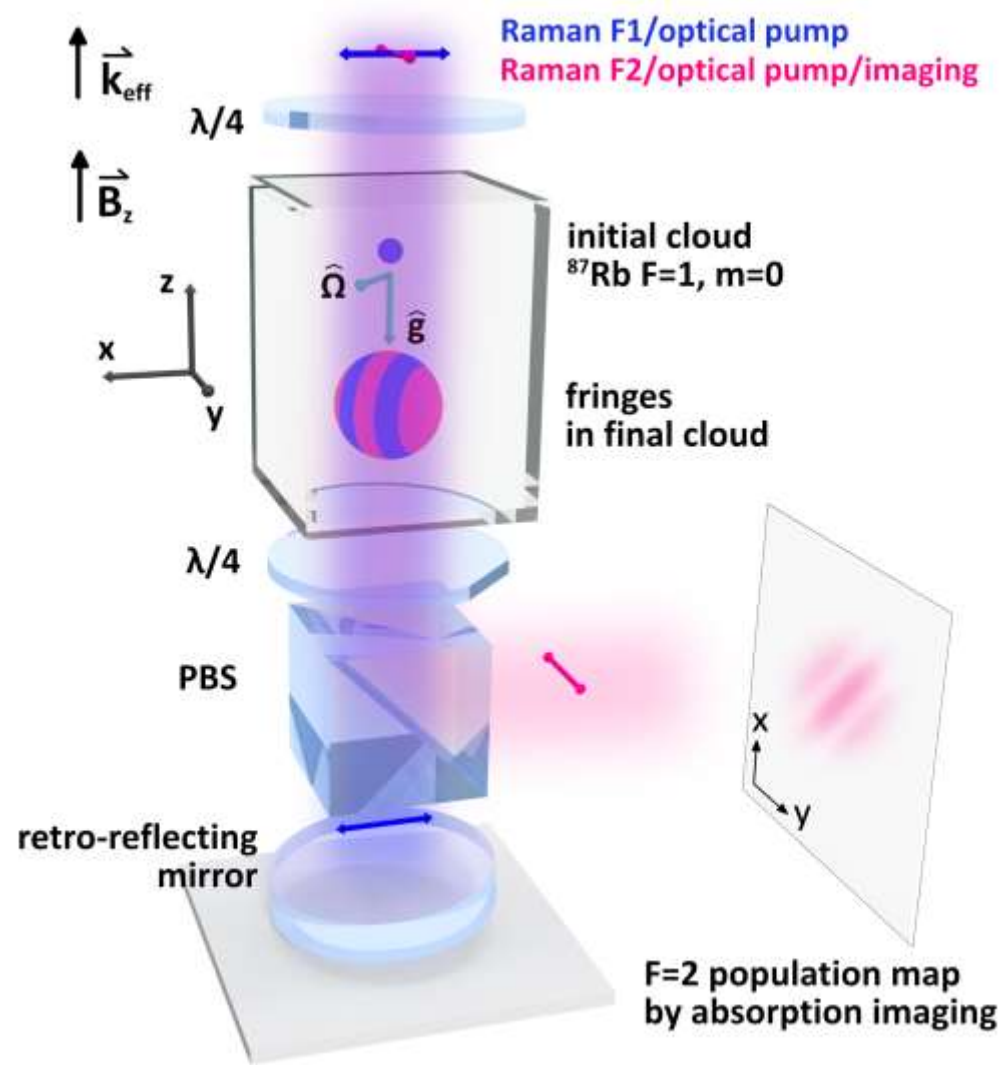
NIST ADI group's PSI gyro

Experimental scheme:

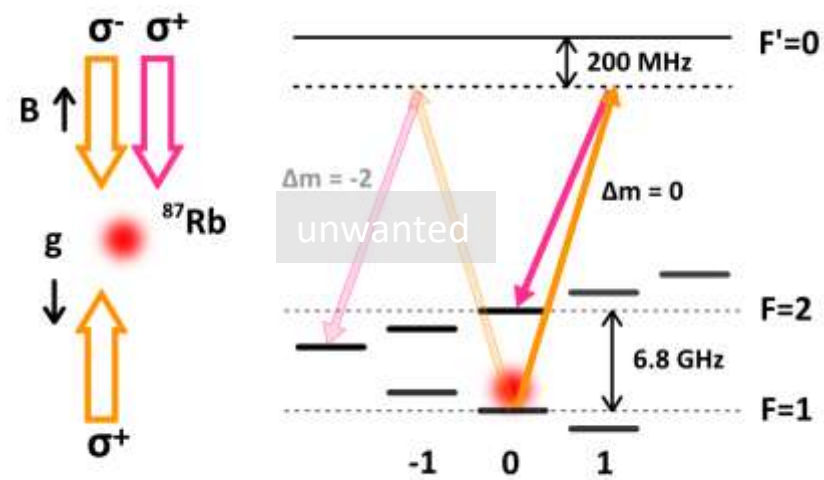
1. MOT, compressed MOT, and molasses
2. State preparation
3. Raman interrogations
4. State-selective absorption imaging

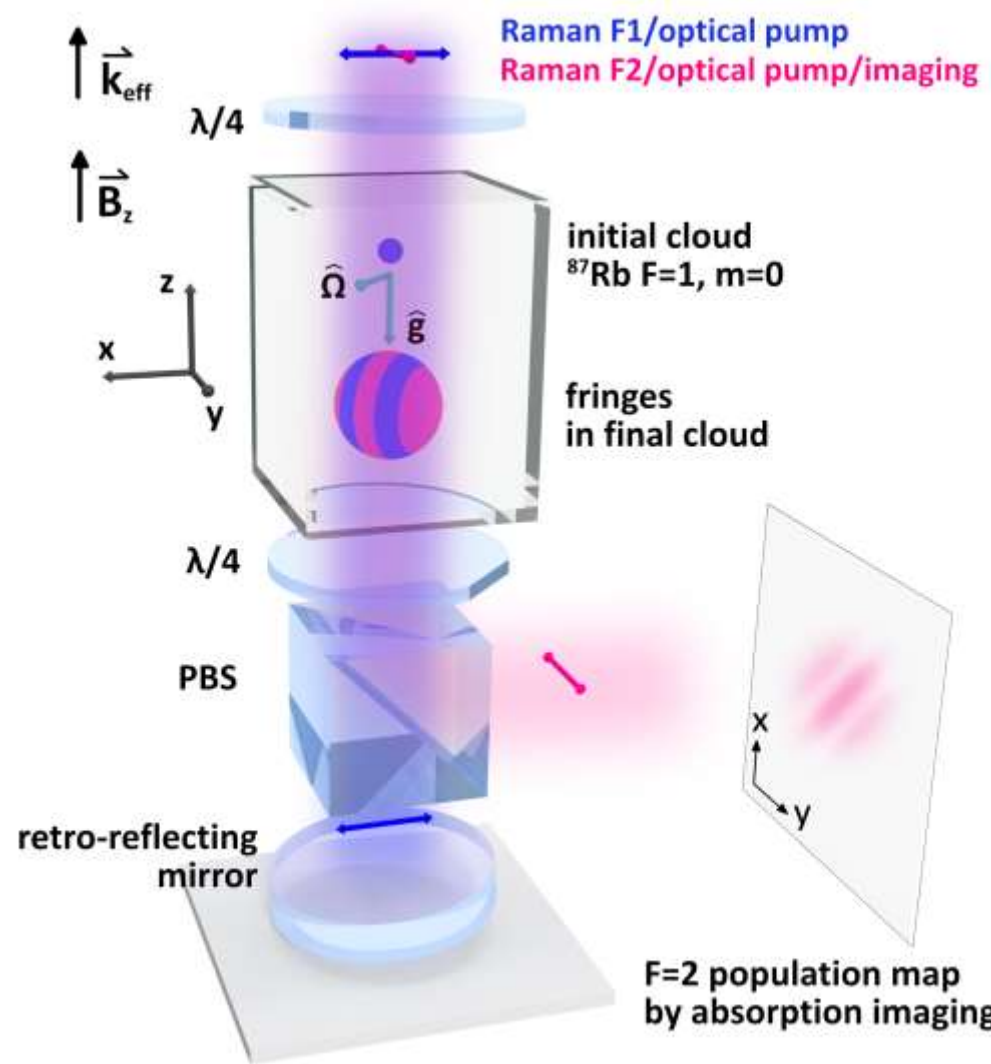
Repetition rate: 5 to 10 Hz





two-photon Raman transition

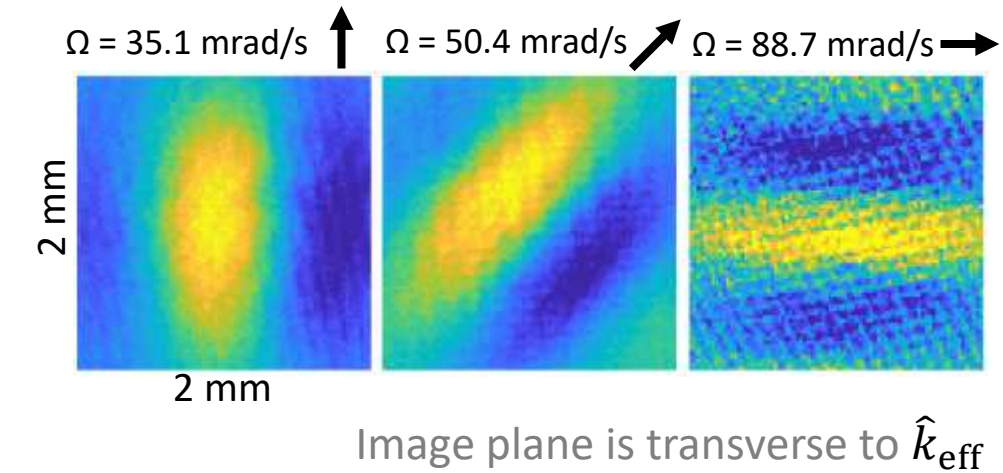




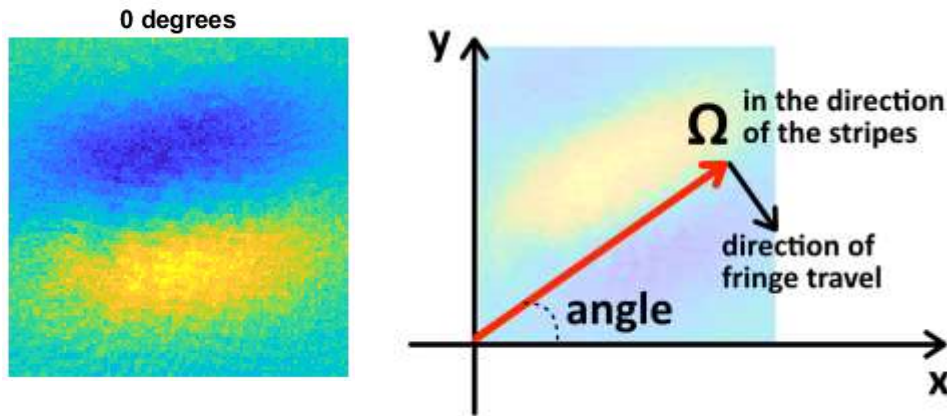
Multi-axis sensitivity

The effective wave vector k_{eff} is in $+z$ direction. Cloud is imaged in xy -plane.
PSI measures:

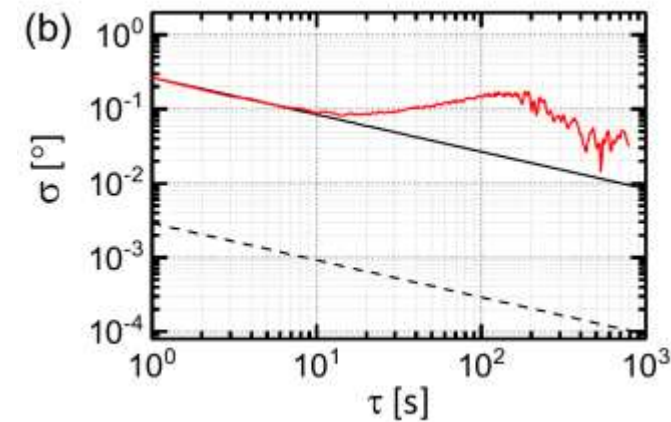
1. Acceleration in the z -axis
2. Rotation projected onto the xy -plane



Experimental demonstration of the two-dimensional rotation measurement with point source atom interferometry



- Fringe period : rotation rate
- Fringe direction : direction of the rotation vector
- Fringe phase : acceleration



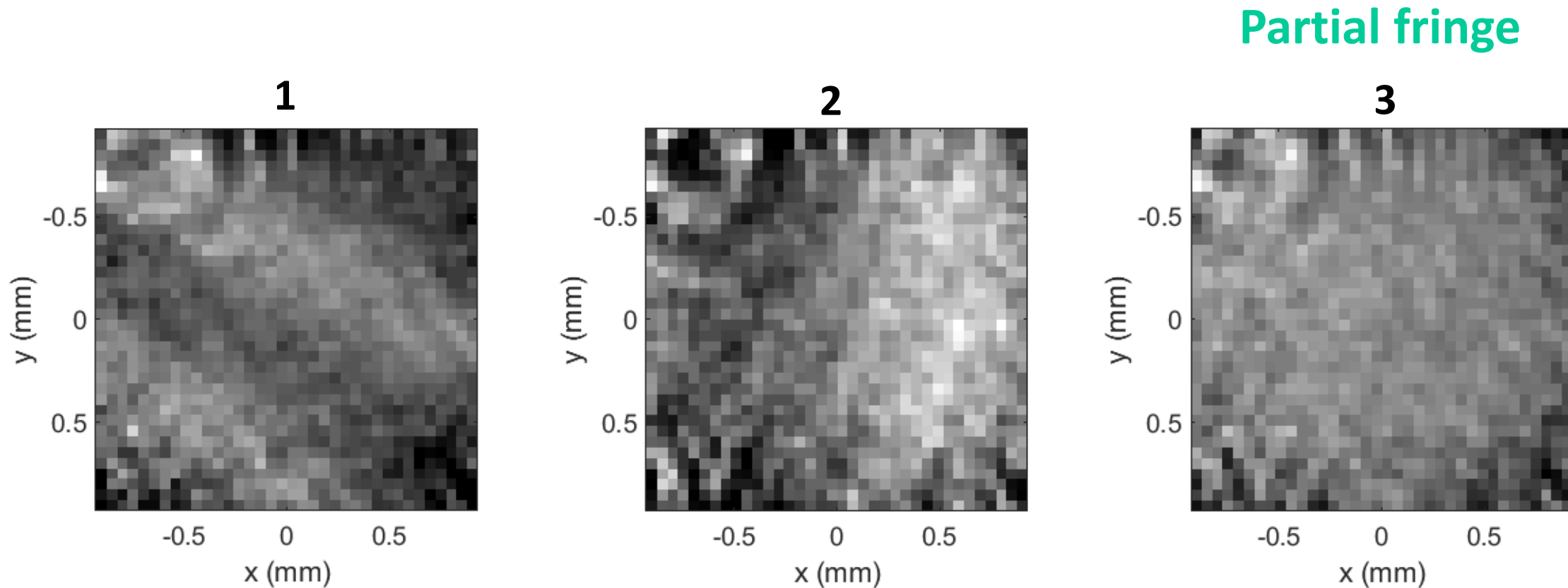
**Direction of the rotation vector
in a plane, 0.27° at $\tau = 1\text{ s}$**

doi.org/10.1103/PhysRevApplied.12.014019

Application ideas:

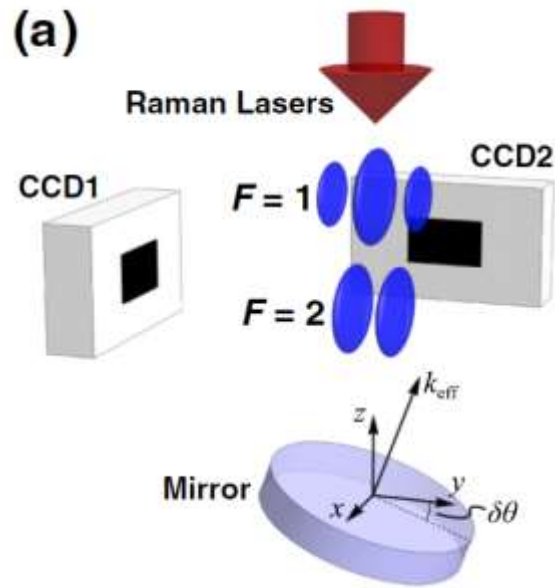
1. navigation, gyrocompassing
2. Fundamental physics, relativistic precession measurement

Measurement of small rotation rates

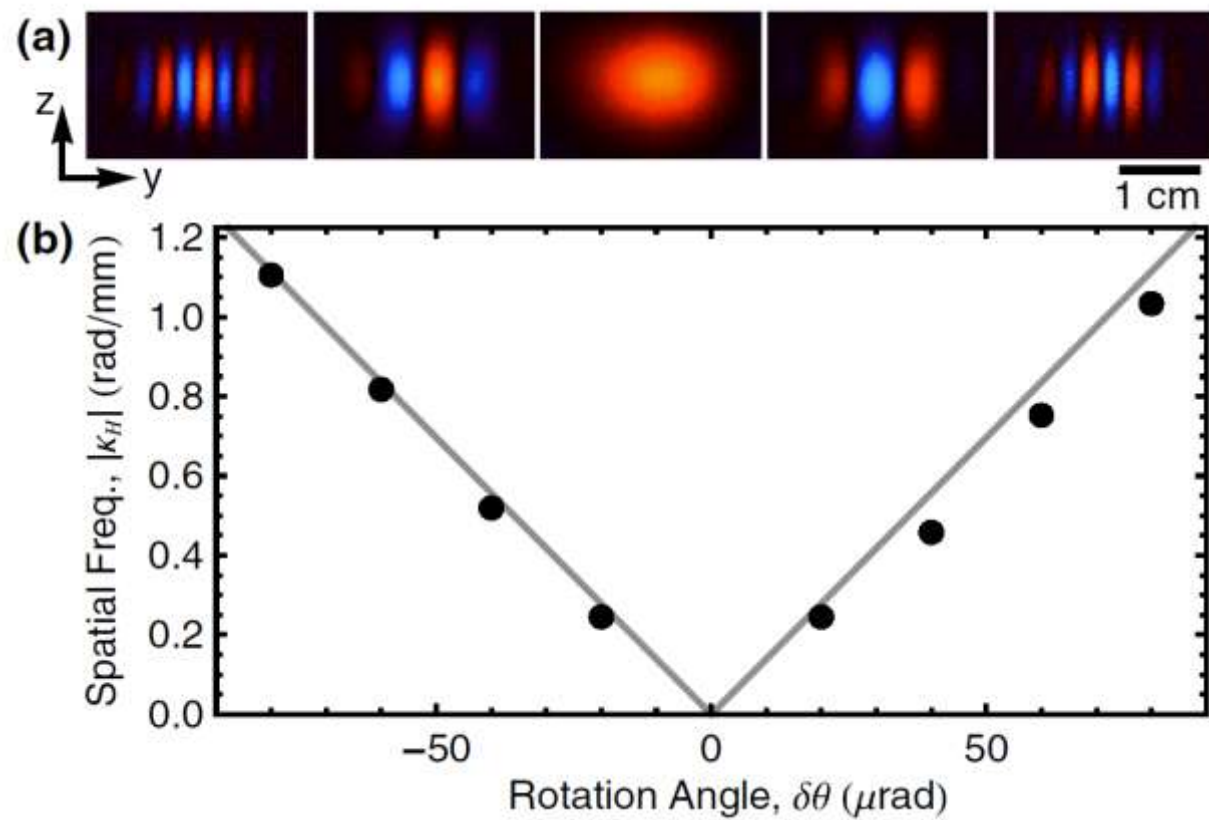


How to measure rotation in case 3?

Method in literature: phase shear



"Enhanced Atom Interferometer Readout through the Application of Phase Shear," A. Sugarbaker, S. M. Dickerson, J. M. Hogan, D. M. S. Johnson, and M. A. Kasevich, PRL **111**, 113002 (2013).



Method in literature: ellipse fitting

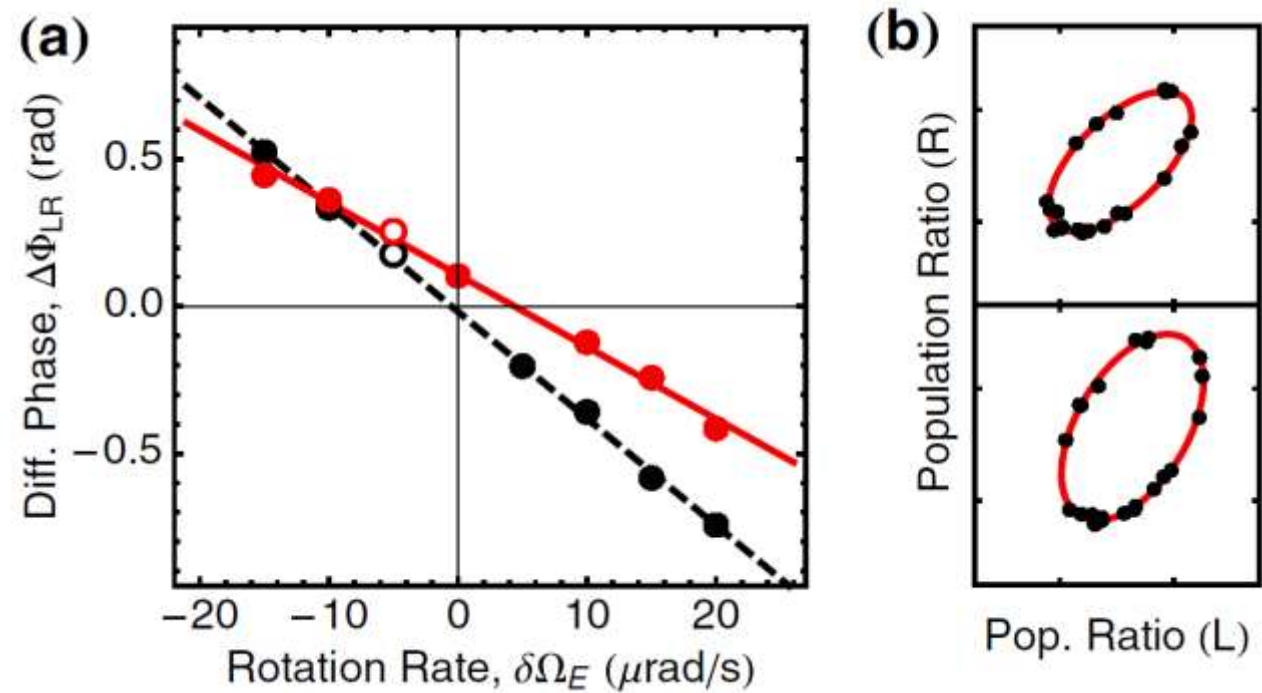
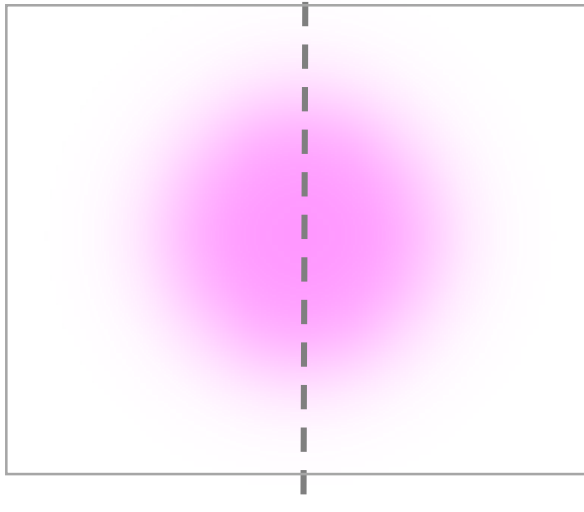
Ellipse equation:

$$Ax^2 + Bxy + Cy^2 + Dx + Ey + F = 0$$

Phase difference:

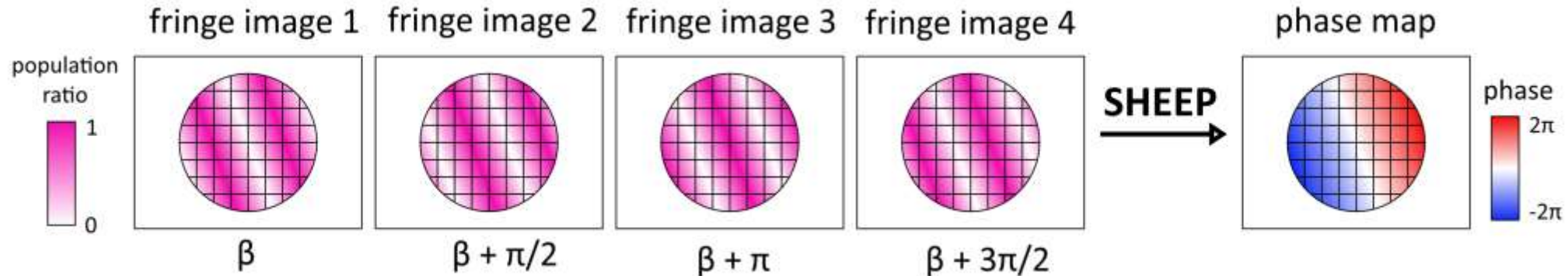
$$\Delta\Phi_{LR} = \cos^{-1}(-B/2\sqrt{AC})$$

Left population ratio = x | Right population ratio = y



“Multiaxis Inertial Sensing with Long-Time Point Source Atom Interferometry,” S. M. Dickerson, J. M. Hogan, A. Sugarbaker, D. M. S. Johnson, M. A. Kasevich, PRL **111**, 083001 (2013).

Our approach

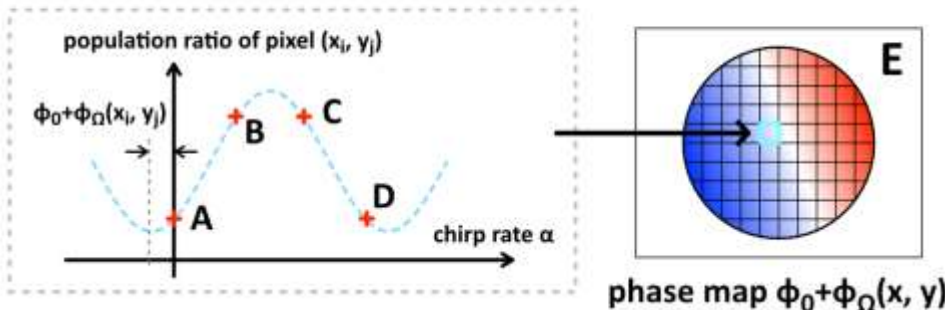
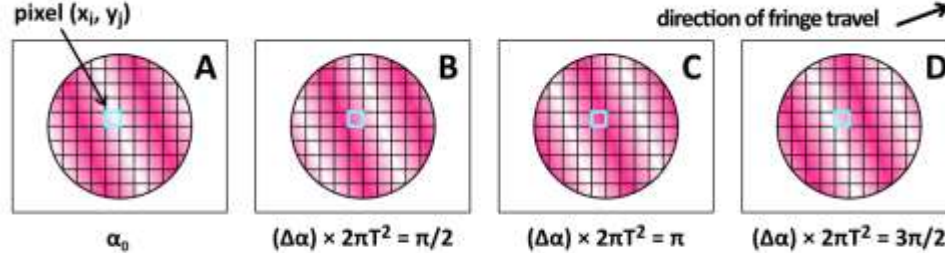


SHEEP—Simple, High dynamic range, and Efficient Extraction of Phase map

<https://doi.org/10.1364/OE.399988>

Phase shifting interferometry

four population ratio images



INPUT

Population ratio maps:

$$A(x_i, y_j) = \frac{1}{2} \{1 - c \cos[\varphi_0 + \varphi_\Omega(x_i, y_j)]\}$$

$$B(x_i, y_j) = \frac{1}{2} \{1 + c \sin[\varphi_0 + \varphi_\Omega(x_i, y_j)]\}$$

$$C(x_i, y_j) = \frac{1}{2} \{1 + c \cos[\varphi_0 + \varphi_\Omega(x_i, y_j)]\}$$

$$D(x_i, y_j) = \frac{1}{2} \{1 - c \sin[\varphi_0 + \varphi_\Omega(x_i, y_j)]\}$$

OUTPUT

Phase map

$$E(x_i, y_j) = \tan^{-1} \frac{B(x_i, y_j) - D(x_i, y_j)}{C(x_i, y_j) - A(x_i, y_j)} + m\pi$$

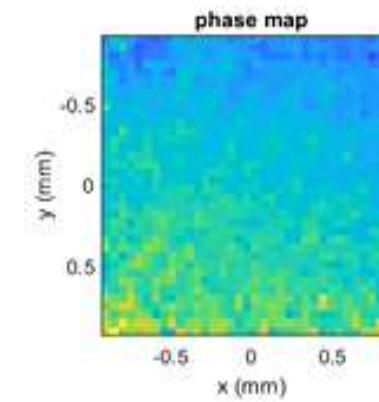
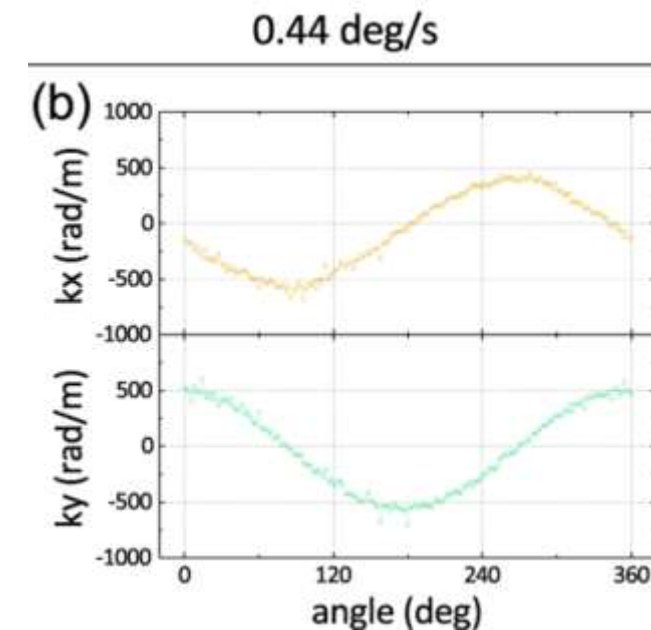
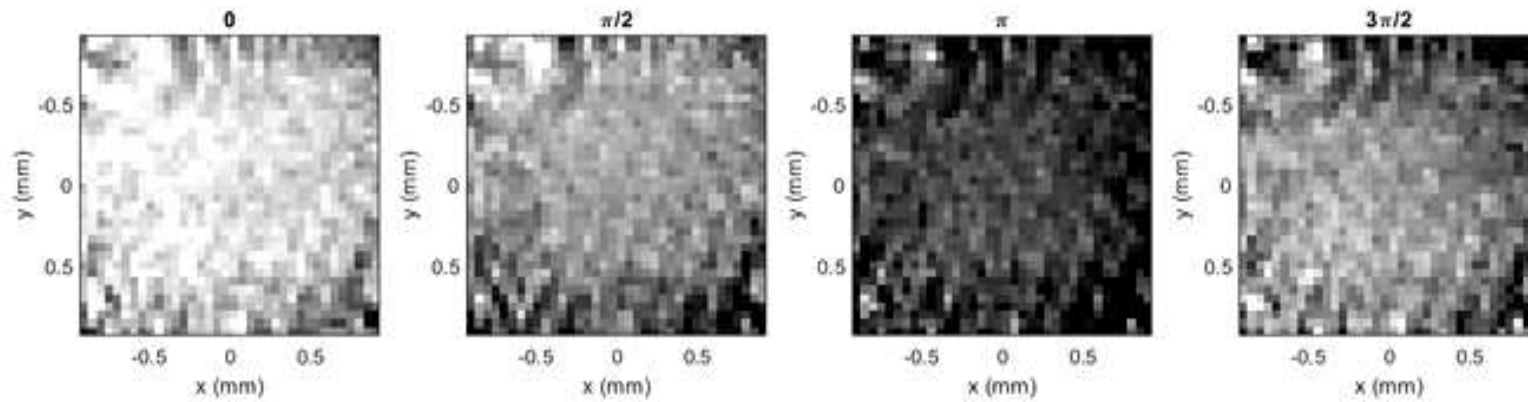
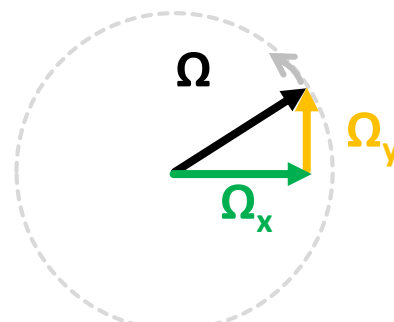
↑
Stitching the
 \tan^{-1} output

$$= \varphi_0 + \varphi_\Omega(x_i, y_j)$$

- Rotation phase gradient : average of the differences in pixel values of adjacent pixels
- Acceleration phase : average of the entire phase map

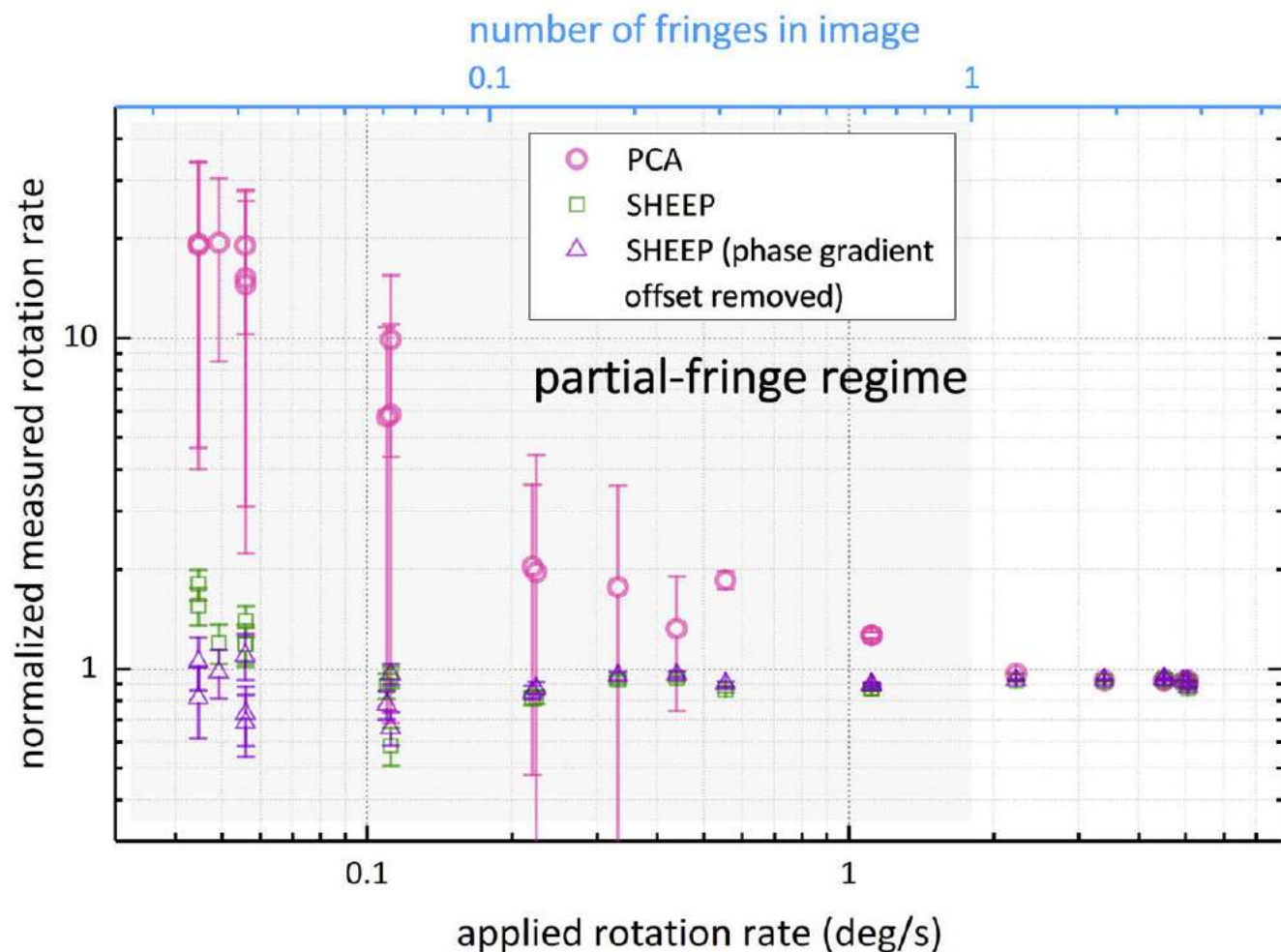
Case 3 revisited with SHEEP method

1. The direction of the rotation traces a 360° range in 2° steps.
2. X- and y- components of the rotation vector vary sinusoidally.



Dynamic range

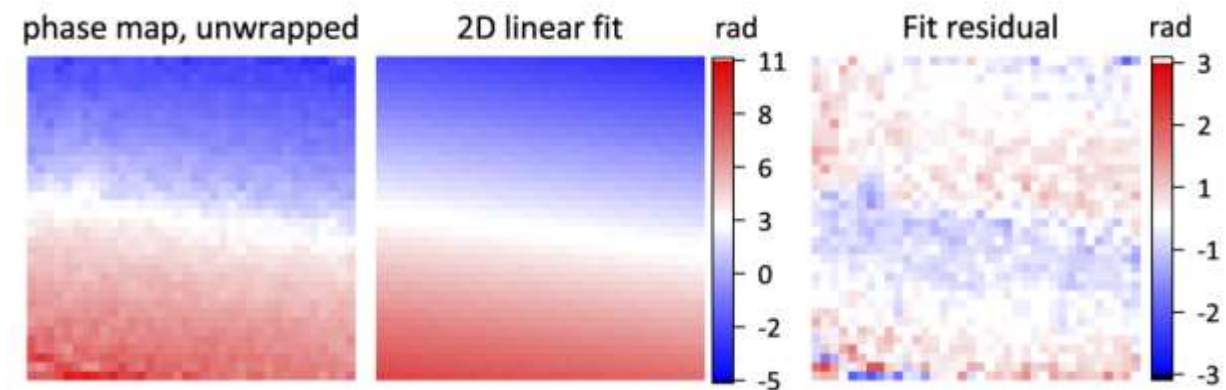
- Robust and accurate
- Performs well over a wide range of rotation rates
- Lowest rotation rate $0.045^\circ/\text{s}$ at $T = 7.8 \text{ ms}$, corresponding to 0.025 fringes in the image.



Discussion

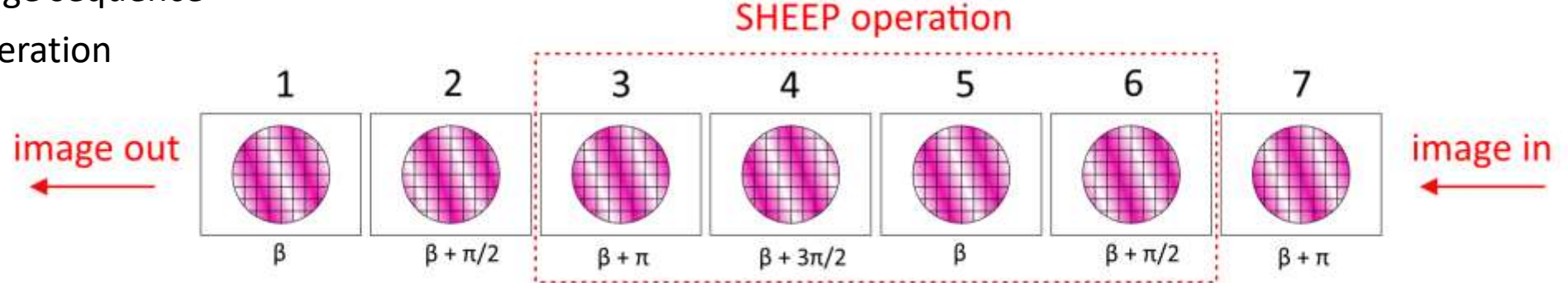
1. Vibrations

- Spurious phase between images
- Sensitivities:
 - Acceleration $\propto T^2$
 - Rotation $\propto T$
- Closed-loop operation



2. Bandwidth

- Three-image sequence
- Queue operation



Conclusions:

1. PSI is simple compared to other atom interferometer techniques.
2. PSI measures two rotation components and one acceleration component at the same time.
3. PSI enables rotation measurement without ambiguity.
4. PSI has a high dynamic range.
5. The SHEEP method returns a phase map with rotation and acceleration information.
6. The SHEEP method does not require a contrast calibration, and it is applicable from the multiple-fringe regime well into the partial-fringe regime.

